



Figures and figure supplements

The transcription factor Bach2 negatively regulates murine natural killer cell maturation and function

Shasha Li et al

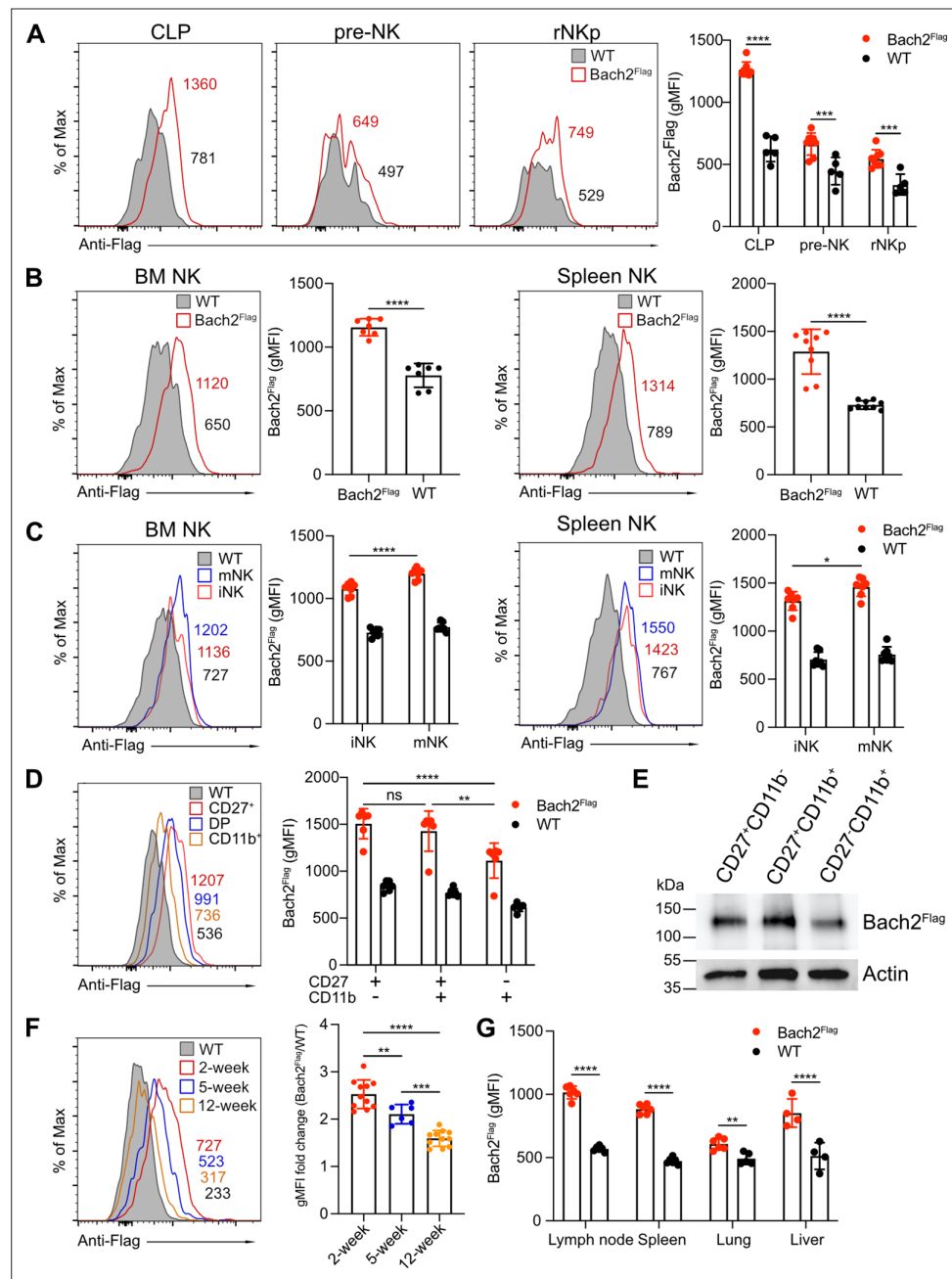


Figure 1. BTB domain And CNC Homolog 2 (Bach2) expression at different natural killer (NK) cell developmental stages by analysis of Bach2^{Flag} knock-in mouse. **(A)** Histogram plots of Bach2^{Flag} expression (red) in common lymphoid progenitor (CLP), pre-NK progenitor (pre-NK), and refined NK progenitor (rNKp) as compared to cells from wild-type (WT) mice (gray fill). The geometric MFI (gMFI) number was indicated in the plot. Summary of gMFI was shown (n=5 for each group in three independent experiments). **(B)** Histogram plots of Bach2^{Flag} expression (red) in NK cell (CD3⁺CD19⁺NK1.1⁺) from bone marrow (BM) and spleen as compared to cells from WT mice (gray fill). Numbers indicate gMFI and summary of gMFI is shown (n=7 or 9 for each group in three to four independent experiments). **(C)** CD3⁺CD122⁺ NK cells from BM and spleen were subdivided into iNK (DX5⁺NK1.1⁺) and mNK (DX5⁺NK1.1⁻) and analyzed for Bach2^{Flag} expression (red for iNK, blue for mNK) as compared to cells from WT mice (gray fill). Numbers indicate gMFI and summary of gMFI is shown (n=7 for each group in three to four independent experiments). **(D)** Histogram plot of Bach2^{Flag} expression in CD27⁺CD11b⁻ (red), CD27⁺CD11b⁺ (blue), and CD27⁻CD11b⁺ (yellow) NK subsets as compared to cells from WT mice (gray fill). Note that WT plot represents expression of Bach2^{Flag} from CD27⁺CD11b⁺ subsets. Numbers indicate gMFI and summary of gMFI is shown (n=6 for each group in three independent experiments). **(E)** Splenic NK cells were sorted into CD27⁺CD11b⁻, CD27⁺CD11b⁺, and CD27⁻CD11b⁺ subsets. *Figure 1 continued on next page*

Figure 1 continued

CD27⁺CD11b⁺ and CD27⁻CD11b⁺ subsets. Bach2^{Flag} expression in the subsets was detected using Anti-FLAG M2-Peroxidase (HRP) antibody by western blot. Expression of Actin was used as an internal control. Two individual experiments have been done with one mouse each time. **(F)** Histogram plot of Bach2^{Flag} expression in splenic NK cell (CD3⁺CD19⁻NK1.1⁺) from mice at 2 weeks' (red), 5 weeks' (blue), and 12 weeks' (orange) age as compared to cells from WT mice (gray fill). Note that WT plot represents expression of Bach2^{Flag} from 12-week age mice. Numbers indicate gMFI and summary of gMFI fold change is shown (n=6 or 11 for each group in three to four independent experiments). **(G)** Summary of gMFI data for Bach2^{Flag} expression in NK cells from lymph node, spleen, lung, and liver (n=4 or 6 for each group in three independent experiments). NK cells from lymph node, spleen, and lung were gated as CD3⁺CD19⁻NK1.1⁺. NK cells from liver were gated as CD3⁺CD19⁻NK1.1⁺DX5⁺. Statistical significance was determined by two-way ANOVA (**A, C, D, and G**), one-way ANOVA, **(F)** or by Student's t test (**B**). Error bars indicate SD. *p<0.05; **p<0.01; ***p<0.001; ****p<0.0001. ns, not significant. See **Figure 1—figure supplement 1** for gating strategies.

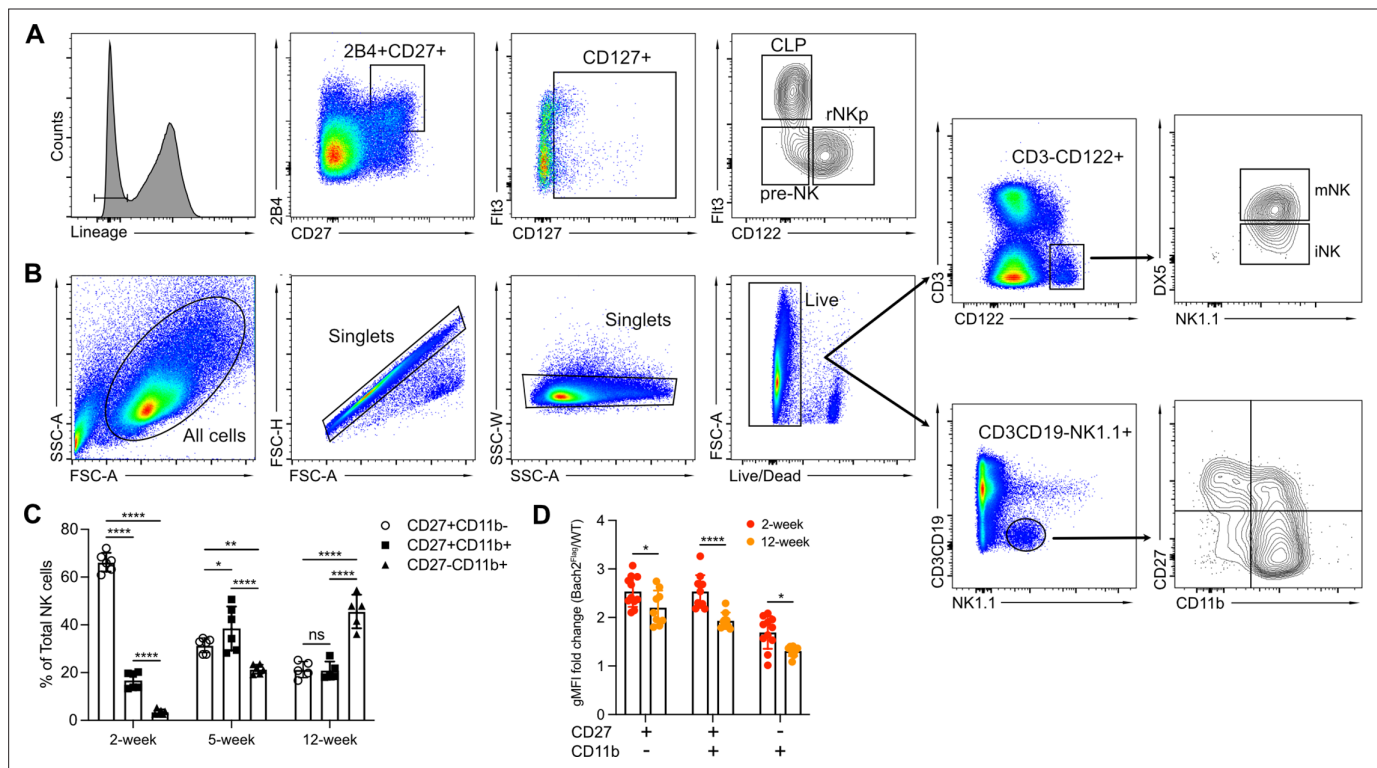


Figure 1—figure supplement 1. Gating strategy for flow cytometry analysis. **(A)** Representative flow cytometry plots show bone marrow (BM) Lin⁻ 2B4⁺CD27⁺CD127⁺ cells were subdivided into common lymphoid progenitor (CLP) (Flt3⁺CD122⁻), pre-natural killer (NK) progenitor (pre-NK) (Flt3⁺CD122⁺), and refined NK progenitor (rNKp) (Flt3⁻CD122⁺) subsets. **(B)** Representative flow cytometry plots show CD3⁺CD122⁺ NK cells were subdivided into immature NK cells (DX5⁻NK1.1⁺) and mature NK cells (DX5⁺NK1.1⁺). Alternatively, CD3⁺CD19⁺NK1.1⁺ NK cells were further subdivided by CD27 and CD11b into maturation subsets. **(C)** Summary of the percentages of CD27⁺CD11b⁻, CD27⁺CD11b⁺, CD27⁻CD11b⁺ NK subsets among total NK cells in 2 weeks', 5 weeks', and 12 weeks' mice (n=5 or 6 for each group in three independent experiments). **(D)** Summary of Bach2^{Flag} geometric MFI (gMFI) fold change in NK cell subsets defined by CD27 and CD11b expression from 2- and 12-week mice (n=9 or 11 for each group in four independent experiments). Statistical significance was determined by two-way ANOVA. Error bars indicate SD. *p<0.05; **p<0.01; ***p<0.001; ****p<0.0001. ns, not significant.

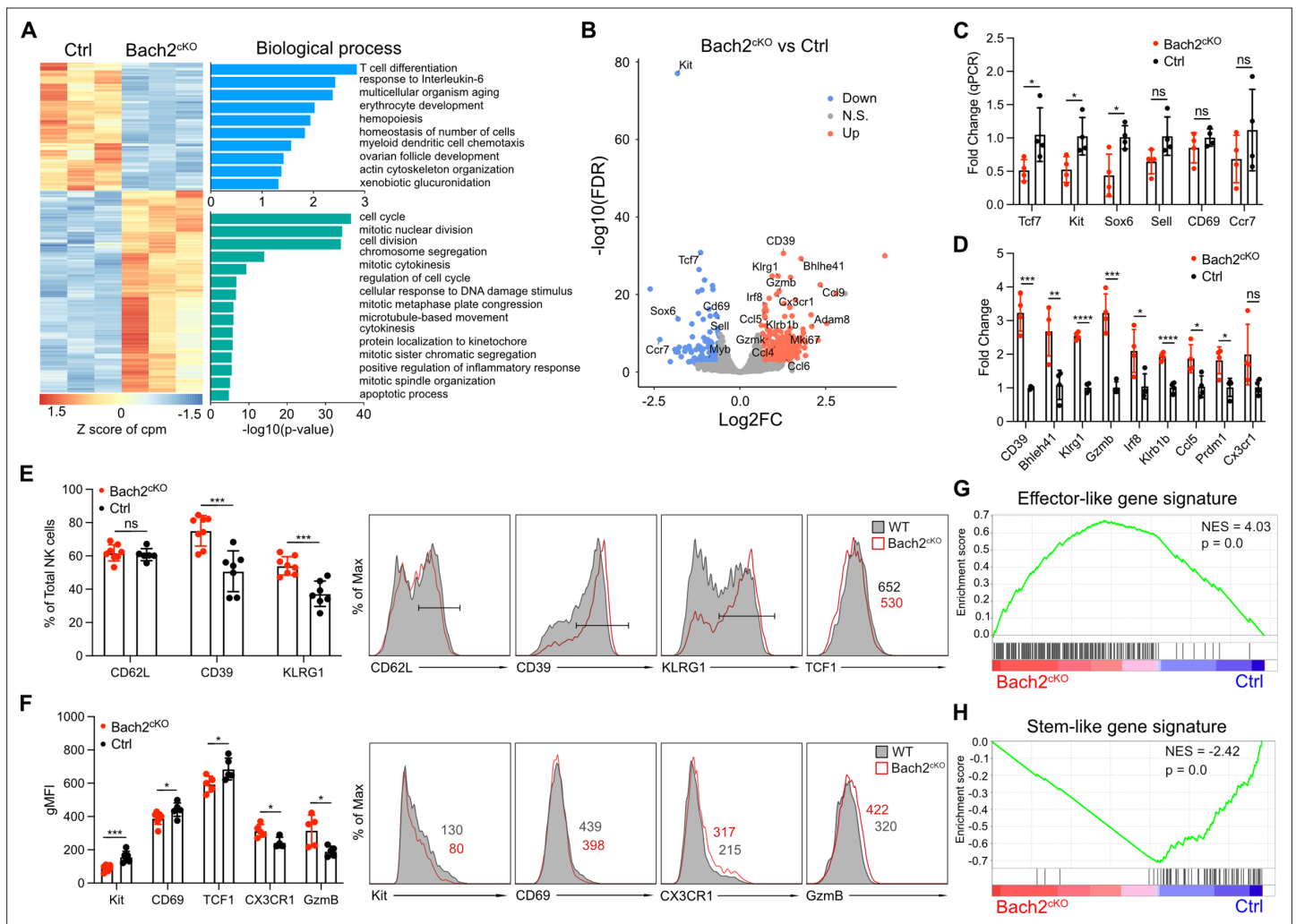


Figure 2. RNA-seq analysis reveals BTB domain And CNC Homolog 2 (*Bach2*) deficiency in natural killer (NK) cells promotes the terminal maturation of NK cells with elevated effector function. **(A)** Heatmap of differentially expressed genes in NK cells compared between control and *Bach2^{ckO}* mice in RNA-seq analysis (FDR < 0.01 and log₂ fold change > 1.5). Each column represents total splenic CD3⁺CD19⁺NK1.1⁺NKp46⁺ cells from an individual mouse. Three biological replicates per group from two individual sorting experiments are shown. The data were analyzed with the Database for Annotation, Visualization and Integrated Discovery (DAVID) Gene Ontology (GO) analysis for the biological process using the genes differentially expressed from NK cells between control and *Bach2^{ckO}* mice. **(B)** Volcano plot shows differential gene expression between control and *Bach2^{ckO}* splenic NK cells. Highlighted are genes discussed in the text. **(C and D)** RNA expression of indicated genes in *Bach2^{ckO}* mice or control mice determined by quantitative PCR (qPCR). Data are shown with four mice per group from two independent experiments. **(E)** Summary of the percentage of NK cells expressing the indicated genes in *Bach2^{ckO}* mice or control mice (n=7 or 8 for each group in three independent experiments). Representative histogram plots show the expression of indicated protein in NK cells from *Bach2^{ckO}* mice (red) as compared to NK cells from control mice (gray fill). **(F)** Summary of the geometric MFI (gMFI) of indicated gene in total NK cells in *Bach2^{ckO}* mice or control mice (n=5–8 for each group in three independent experiments). Representative histogram plots show the expression of indicated proteins in NK cells in *Bach2^{ckO}* mice (red) as compared to NK cells from control mice (gray fill). **(G and H)** Gene set enrichment analysis (GSEA) illustrating enrichment of effector-like **(G)** and stem-like **(H)** gene signatures in *Bach2^{ckO}* and control splenic NK cells. Statistical significance was determined by Student's t test. Error bars indicate SD. *p<0.05; **p<0.01; ***p<0.001; ****p<0.0001. ns, not significant.

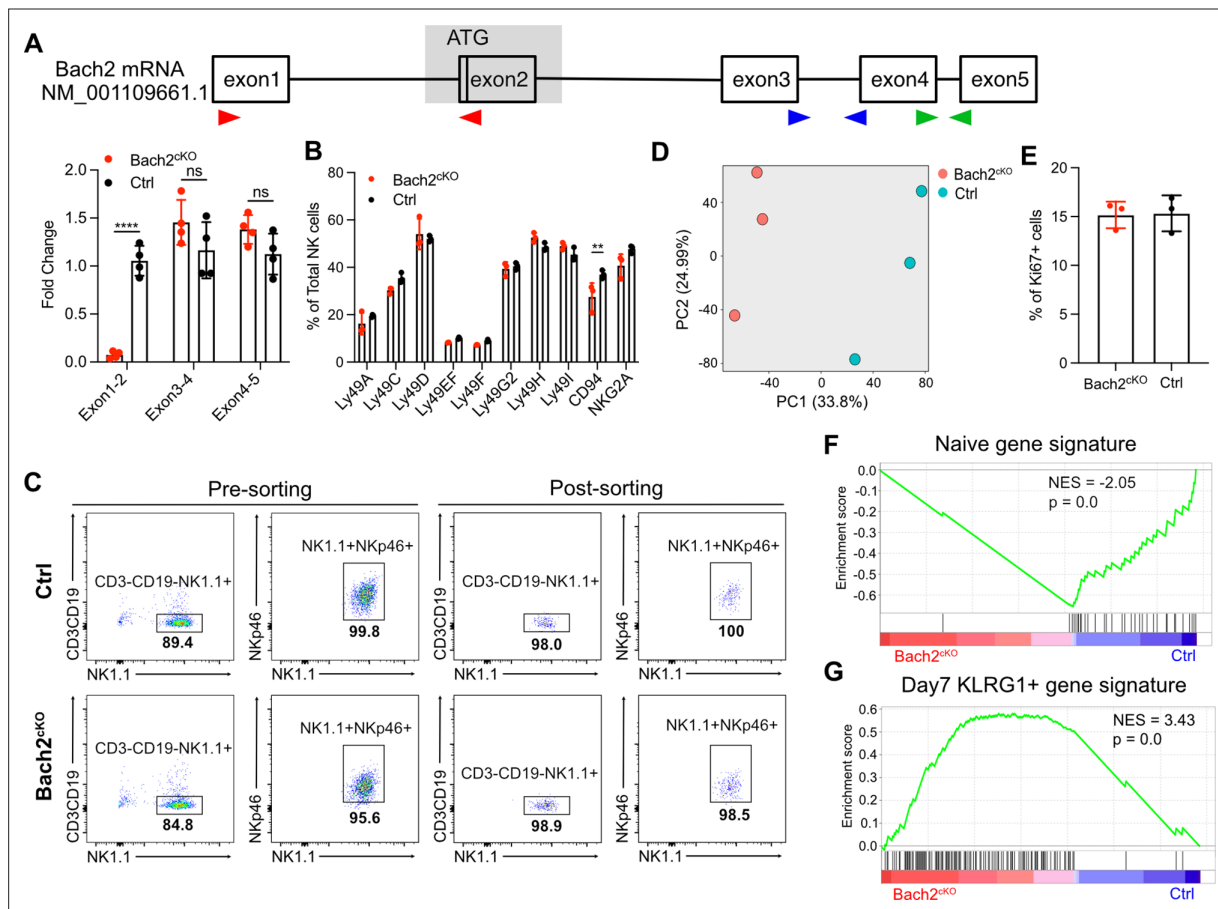


Figure 2—figure supplement 1. BTB domain And CNC Homolog 2 (*Bach2*) deficiency in natural killer (NK) cells resemble activated effector CD8⁺ T cells. **(A)** Schematic plot shows quantitative PCR (qPCR) primers targeting regions on *Bach2* mRNA. Red arrows represent primers targeting exon 1 to exon 2. Blue arrows represent primers targeting exon 3 to exon 4. Green arrows represent primers targeting exon 4 to exon 5. The gray box denotes the region that has been deleted. RNA expression of *Bach2* was determined by qPCR with the indicated exon primer sets. Data are shown with four mice per group from two independent experiments. **(B)** Summary of the expression profile of various NK receptors (% of total NK cells) in control and *Bach2^{CKO}* mice (n=3 for each group in three independent experiments). **(C)** Flow cytometry sorting of splenic NK cells (CD3⁺CD19⁻NK1.1⁺NKp46⁺) from *Bach2^{CKO}* or control mice for RNA-seq analysis. Post-sorting flow cytometry shows the purity of the NK cells. **(D)** Principal component analysis (PCA) of differentially expressed genes (log₂ fold change > 1.5 and FDR < 0.01 or log₂ fold change < -1.5 and FDR < 0.01) for splenic NK cells isolated from control and *Bach2^{CKO}* mice. **(E)** Summary of Ki67⁺ cells in *Bach2^{CKO}* mice or control mice (n=4 for each group in three independent experiments). **(F and G)** Gene set enrichment analysis (GSEA) plots illustrate the enrichment of naïve **(F)** and day 7 after infection with rVV-OVA KLRG1⁺ positive **(G)** CD8⁺ T cells gene signatures (Roychoudhuri et al., 2016a) in *Bach2^{CKO}* and control splenic NK cells. Statistical significance was determined by two-way ANOVA. Error bars indicate SD. **p < 0.01; ****p < 0.0001. ns, not significant.

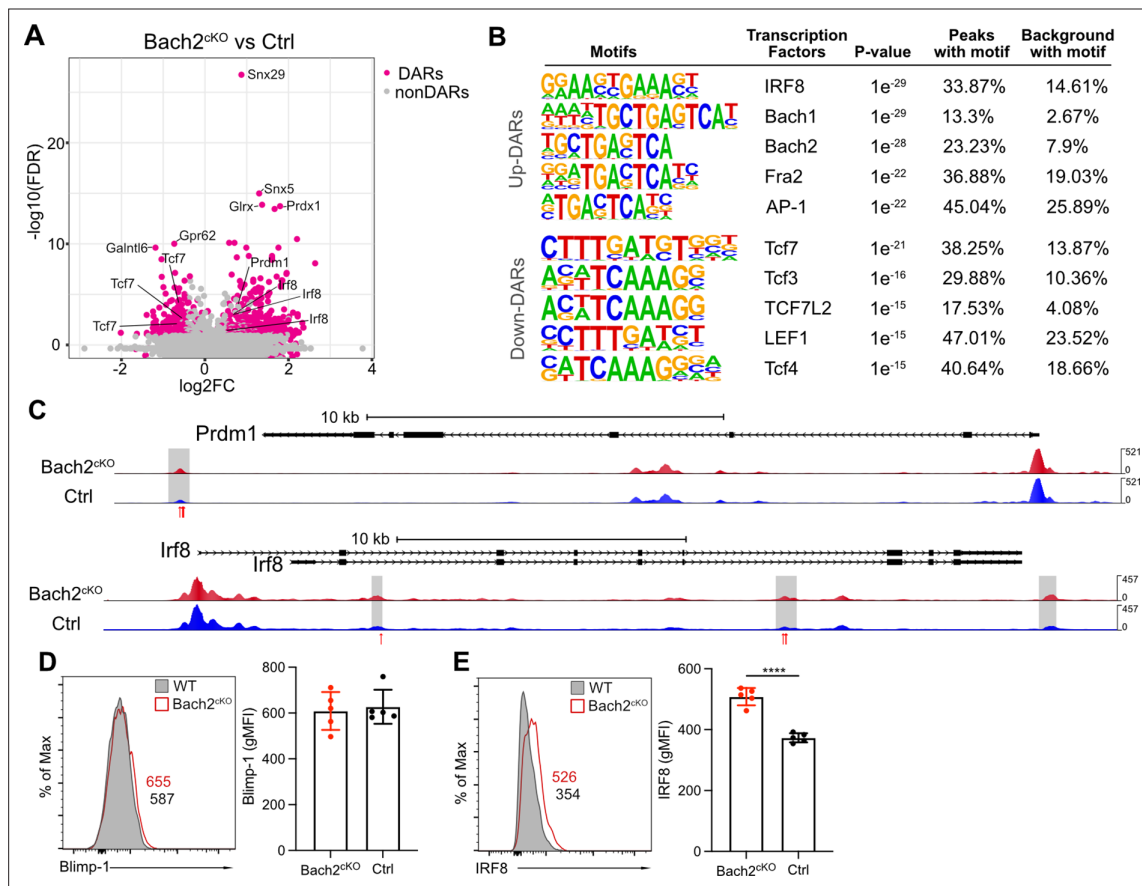


Figure 3. Bach2 deficiency results in increased accessible regions in the genome of natural killer (NK) cells. **(A)** Volcano plot shows the differentially accessible regions (DARs) and non-DARs between control and Bach2^{ckO} splenic NK cells. **(B)** De novo motif enrichment at regions of open chromatin as defined by assay for transposase-accessible chromatin coupled with high throughput sequencing (ATAC-seq) in splenic NK cells from Bach2^{ckO} mice compared to cells from control mice. Motifs of interest are listed. **(C)** Genome browser visualization of ATAC-seq peak near *Prdm1* and *Irf8* gene loci in NK cells from Bach2^{ckO} mice (red) and control mice (blue). Gray boxes denote differential accessible regions. Red arrows show the location of Bach2-binding motif. **(D and E)** Histogram plot shows the expression of Blimp-1 **(D)** and IRF8 **(E)** in NK cells from Bach2^{ckO} mice (red) as compared to control mice (gray fill). Numbers indicate geometric MFI (gMFI). Summary of gMFI is shown (n=5 for each group in three independent experiments). Statistical significance was determined by Student's t test. Error bars indicate SD. *p<0.05; ****p<0.0001.

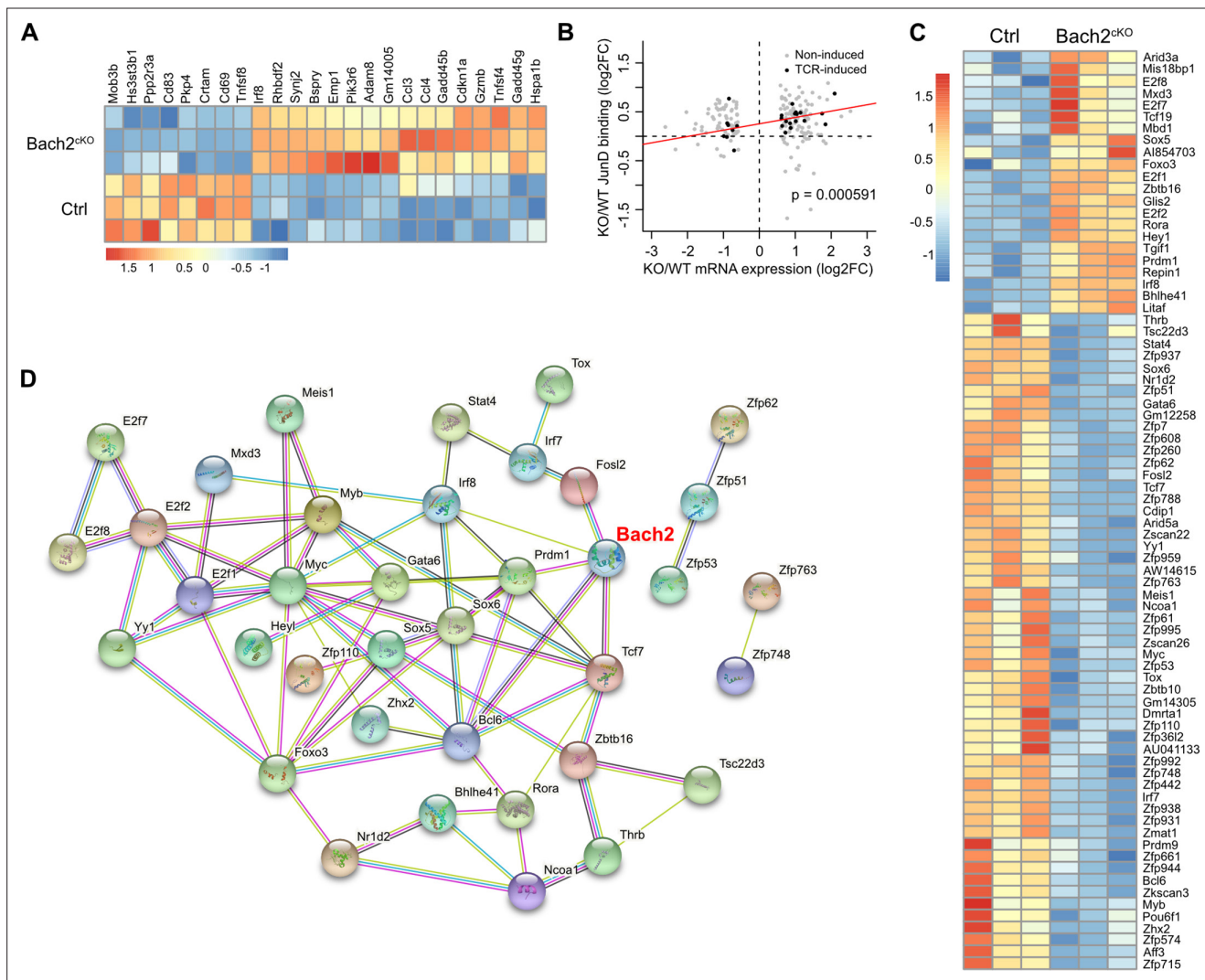


Figure 3—figure supplement 1. Potential protein interactions between BTB domain And CNC Homolog 2 (Bach2) and differentially regulated transcription factors in natural killer (NK) cells. **(A and B)** Differentially expressed genes in NK cells between Bach2^{CKO} mice and control mice were compared for genes that were recognized as Bach2 target genes in CD8⁺ T cells (*Roychoudhuri et al., 2016a*). The TCR-induced gene list was used for comparison. Heatmap of the overlapped genes is shown **(A)**. Differences between average JunD binding at Bach2-binding sites (data from published CD8⁺ T cells) with differences in mRNA expression of associated genes in NK cells **(B)**, using the ratios of Bach2^{CKO}/WT JunD-binding versus expressed genes. All Bach2 target genes in CD8⁺ T cells including TCR-induced genes and non-TCR-induced genes were used to compare by exact two-sample Kolmogorov-Smirnov test. lm method was used to add the red line. **(C)** Heatmap of differentially expressed transcription factors in NK cells comparing control and Bach2^{CKO} mice in RNA-seq analysis (FDR < 0.05 and log2 fold change > 0.2). **(D)** Protein interaction between the differentially expressed transcription factors analyzed at the website STRING (<https://string-db.org>). Disconnected nodes in the network were hidden.

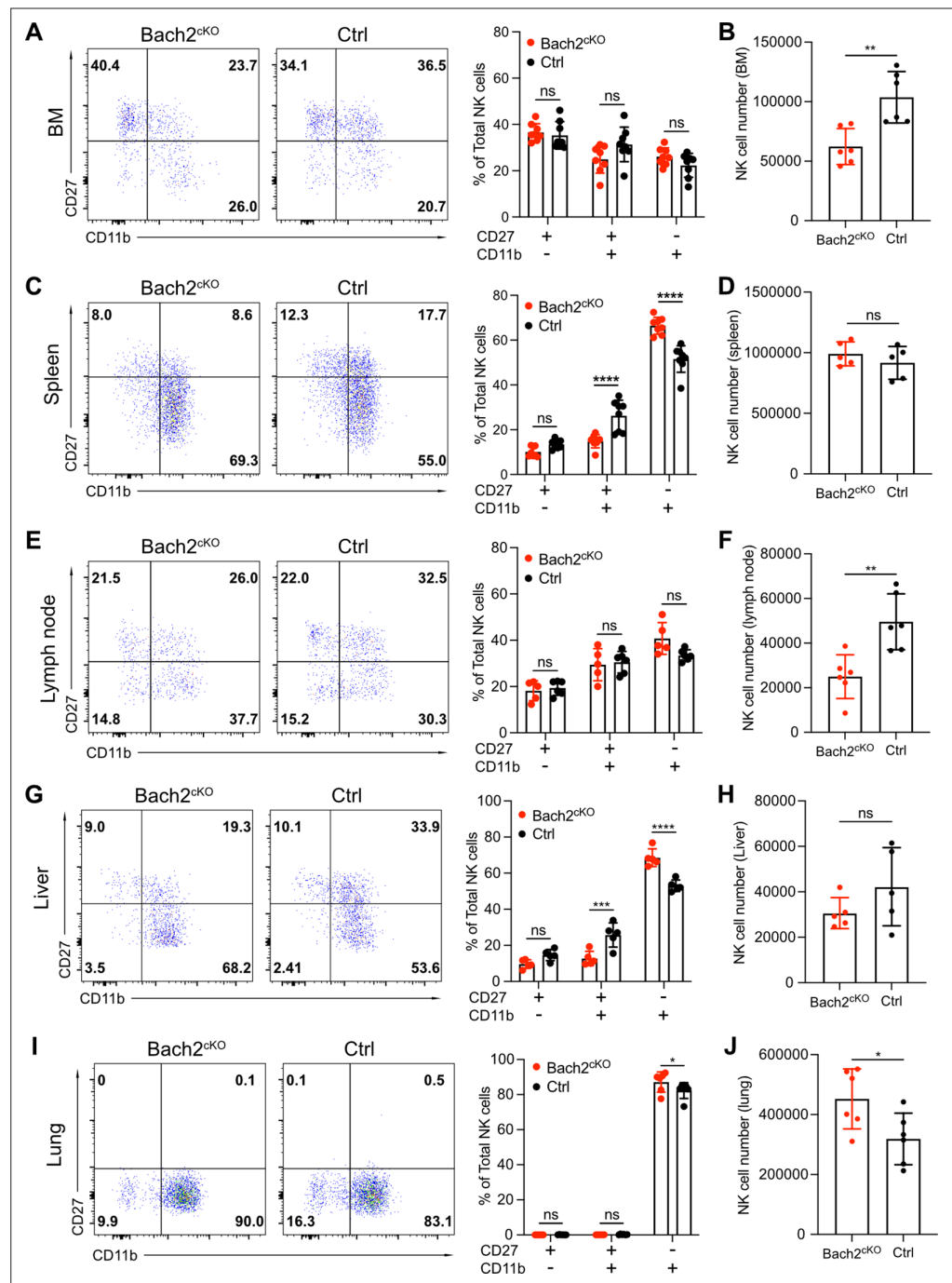


Figure 4. Bach2 deficiency increases natural killer (NK) cells with terminally differentiated phenotype. Representative flow cytometry plots show NK cells (CD3⁺CD19⁻NK1.1⁺NKP46⁺) separated into maturation stages by CD27 and CD11b expression. The percentage of CD27⁺CD11b⁻, CD27⁺CD11b⁺, CD27⁻CD11b⁺ NK cells among all NK cells (left, representative flow plots; right, bar graph summary) from bone marrow (BM) (A), spleen (C), lymph node (E), liver (G) and lung (I) in Bach2^{cKO} mice and control mice were plotted (n=5–8 for each group from three independent experiments). Note that NK cells from liver were gated on CD3⁺CD19⁻DX5⁺NK1.1⁺NKP46⁺. Summary of the total number of NK cells from BM (B), spleen (D), lymph node (F), liver (H), and lung (J) in Bach2^{cKO} mice and control mice were plotted (n=5–8 for each group from three independent experiments). Statistical significance was determined by two-way ANOVA (A, C, E, G, and I) or by Student's t test (B, D, F, H, and J). Error bars indicate SD. *p<0.05; **p<0.01; ***p<0.001; ****p<0.0001. ns, not significant.

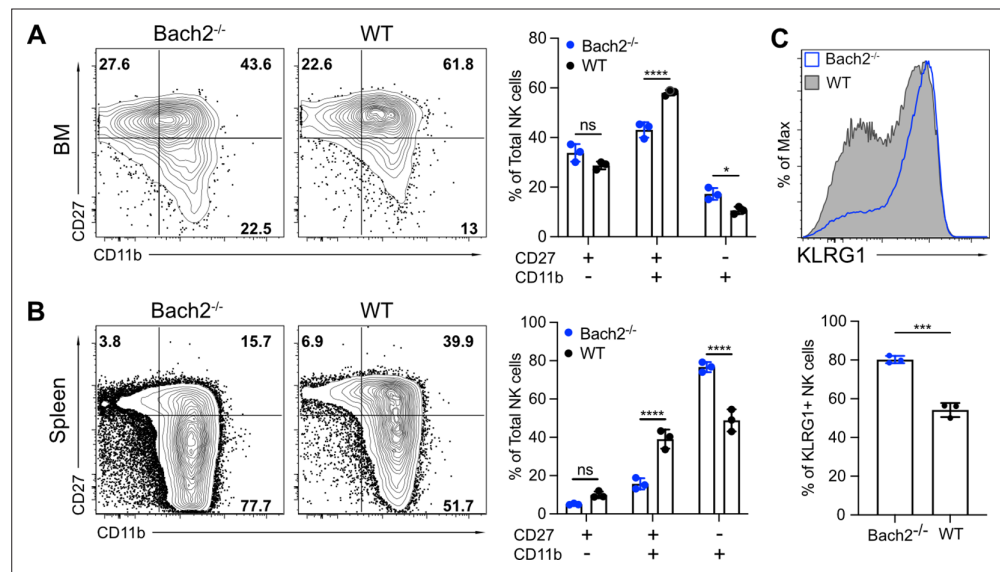


Figure 4—figure supplement 1. BTB domain And CNC Homolog 2 (*Bach2*) deficiency results in a more mature phenotype. **(A and B)** Representative flow cytometry plots and summary of total natural killer (NK) cells ($CD3^-CD19^+NK1.1^+NKp46^+$) maturation stages determined by CD27 and CD11b expression from bone marrow (BM) **(A)** or spleen **(B)** in *Rag1^{-/-}Bach2^{-/-}* (*Bach2^{-/-}*) and *Rag1^{-/-}* (wild-type [WT]) mice. The percentage of different subsets among total NK cells was plotted ($n=3$ for each group in one experiment). **(C)** Representative histogram of KLRG1 expression on splenic NK cells ($CD3^-CD19^+NK1.1^+NKp46^+$) from *Rag1^{-/-}Bach2^{-/-}* (*Bach2^{-/-}*) and *Rag1^{-/-}* (WT) mice. The percentages of NK cells that express KLRG1 are shown in the bar graph ($n=3$ for each group in one experiment). Statistical significance was determined by two-way ANOVA with Bonferroni correction **(A and B)** or by Student's t test **(C)**. Error bars indicate SD. * $p<0.05$; ** $p<0.01$; *** $p<0.001$; **** $p<0.0001$; ns, not significant.

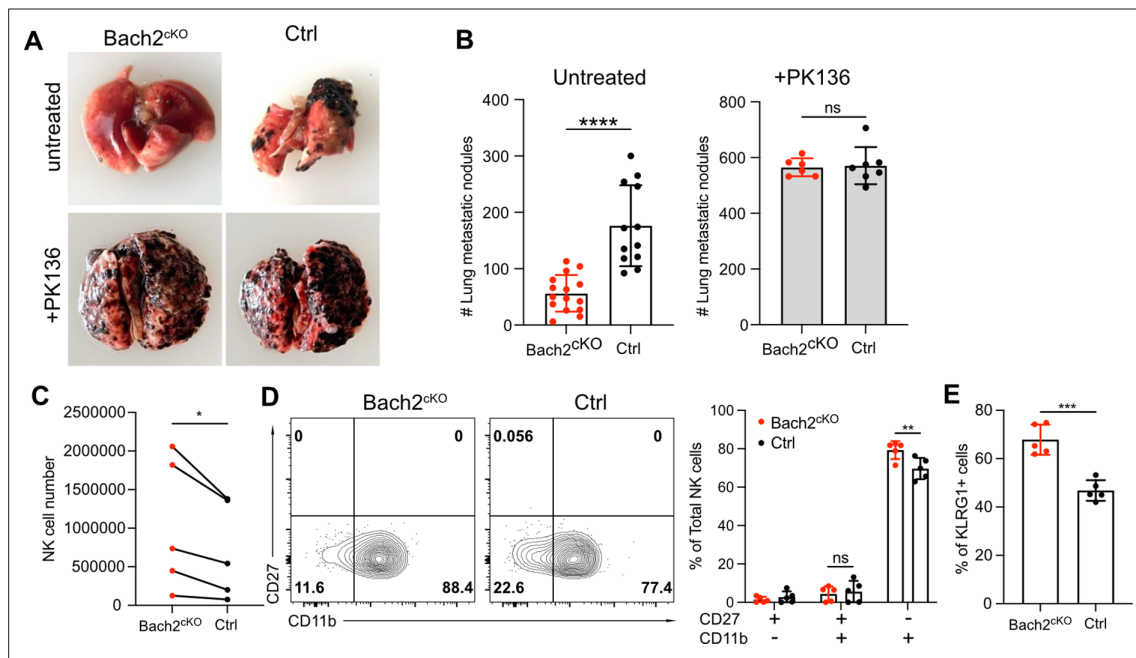


Figure 5. Lack of BTB domain And CNC Homolog 2 (*Bach2*) expression in natural killer (NK) cells suppresses B16F10 tumor metastasis. (A) Representative picture of lung metastatic nodules in *Bach2*^{ckO} mice and control mice under steady-state or anti-NK1.1 (PK136) depletion. (B) Summary of the number of B16F10 metastatic nodules in lung from *Bach2*^{ckO} and control mice with or without anti-NK1.1 (PK136) depletion. Data were pooled from three to four independent experiments with a total of six to fifteen mice per group. (C–E) 2×10^5 B16F10 cells were intravenously injected to *Bach2*^{ckO} mice or control mice. After 24 hr, NK cells from lung were harvested and analyzed for total number (C), maturation by CD27 and CD11b (D), and the percentage of KLRG1⁺ NK cells (E). Average NK cell numbers were calculated for each experiment with one to two mice per group, and data were pooled together from five independent experiments (C). Data were pooled from three independent experiments with five mice per group (D and E). Statistical significance was determined by Student’s t test (B and E), Student’s t test (paired t test) (C), or by two-way ANOVA (D). Error bars indicate SD. * $p < 0.05$; ** $p < 0.01$; *** $p < 0.001$; **** $p < 0.0001$. ns, not significant.

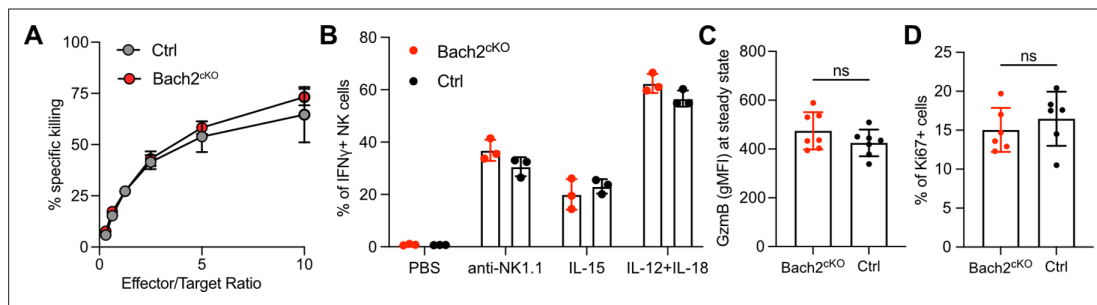


Figure 5—figure supplement 1. Natural killer (NK) cell effector function was unchanged with BTB domain And CNC Homolog 2 (Bach2) deficiency. **(A)** Killing of B16F10 tumor cells by lymphokine-activated killer (LAK) cells from spleen of Bach2^{cKO} mice or control mice. Data are shown as of one representative experiment with three mice per group from three independent experiments. **(B)** Splenocytes from Bach2^{cKO} mice or control mice were treated with anti-NK1.1, IL-15, or IL-12 plus IL-18 and analyzed for interferon- γ (IFN γ) expression. Summary of IFN γ -positive NK cells is shown. Data are shown as of one representative experiment with three mice per group from three independent experiments. **(C)** Summary of GzmB expression in lung NK cells from Bach2^{cKO} mice or control mice at steady state is shown (n=7 for each group in three independent experiments). **(D)** 2×10^5 B16F10 cells were intravenously injected into Bach2^{cKO} mice or control mice. After 24 hr, cells from the lung were harvested and analyzed for Ki67-positive cells. Summary of Ki67-positive NK cells in the lung from Bach2^{cKO} mice or control mice after tumor inoculation (n=6 or 7 for each group in three independent experiments). Statistical significance was determined by Student's t test. Error bars indicate SD. ns, not significant.